CONFERENCE PRE-PRINT

INVESTIGATION OF BROADBAND FLUCTUATION-INDUCED INWARD TRANSPORT AT THE EDGE OF HL-2A NBI HEATED L-MODE PLASMA

Jie Wu

University of Science and Technology of China Hefei, People's Republic of China

Tao Lan

University of Science and Technology of China Hefei, People's Republic of China

Email: lantao@ustc.edu.cn

Weixing Ding

University of Science and Technology of China

Hefei, People's Republic of China

Ge Zhuang

University of Science and Technology of China

Hefei, People's Republic of China

Abstract

The paper report observation of broadband fluctuation-induced inward particle transport at the edge of HL-2A NBI heated L-mode plasmas. The transport direction reversal occurs across a broad frequency spectrum, characterized by significant density fluctuation amplitude variations while radial velocity fluctuations remain relatively stable. The coherence between density and radial velocity fluctuations evolves through a distinct sequence: declining during phase slippage and recovering during phase locking. Both Reynolds stress and radial velocity gradient play crucial roles in driving inward transport. Enhanced Reynolds stress coherency in low-frequency domains indicates improved cross-dimensional turbulence correlation in poloidal and radial directions, essential for effective momentum transfer and inward particle transport. These findings advance understanding of plasma edge dynamics and turbulence-transport interplay, with implications for optimizing plasma confinement in fusion devices.

1. INTRODUCTION

Anomalous transport remains a critical challenge in magnetic confinement fusion, limiting plasma confinement performance. While turbulence typically drives outward transport, counter-gradient inward transport has been observed in various fusion devices. In tokamaks, inward flux often occurs during L-H transitions and has been linked to specific turbulence characteristics.

The fluctuation-induced particle flux can be expressed as:

$$\Gamma_{r,fluc} = \langle \tilde{n}_e \tilde{V}_r \rangle = \frac{\langle \tilde{n}_e^2 \rangle^{1/2} \langle \tilde{E}_{\theta}^2 \rangle^{1/2}}{B_{\phi}} \gamma_{nE} \cos \alpha_{nE},$$

where transport direction depends on the cross-phase α_{nE} between density and electric field fluctuations. Recent research aims to actively reverse transport direction to improve confinement.

This study investigates fluctuation-induced inward particle flux in NBI-heated HL-2A plasmas, focusing on the roles of turbulence coherence, Reynolds stress, and radial velocity gradients in driving inward transport against prevailing density gradients.

2. EXPERIMENTAL SETUP

Experiments were conducted on HL-2A tokamak (R=1.65 m, a=0.4 m) with $B_t = -1.3$ T, $I_p = 150-160$ kA, and line-averaged density $\overline{n} = (1.5 - 2.5) \times 10^{19} \, m^{-3}$. NBI heating (500 kW, 800-1600 ms) was applied.

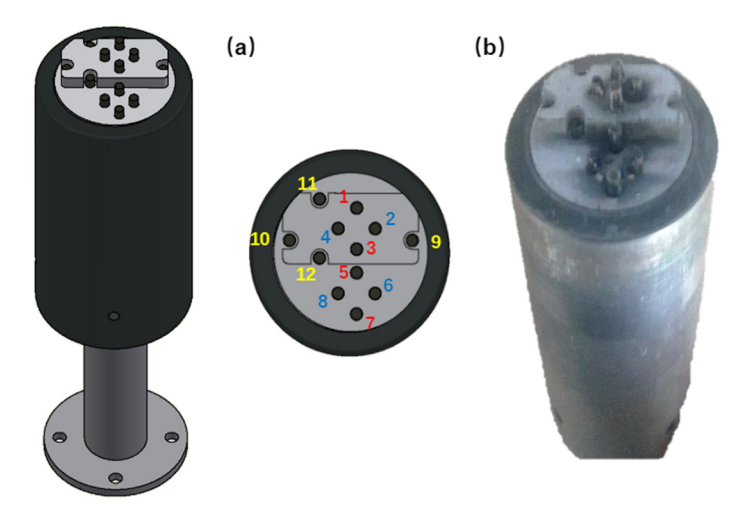


FIG. 1. Schematic of reciprocating Langmuir probe array.

Density and electric field fluctuations were measured using two poloidally separated fast reciprocating Langmuir probe arrays with 1 MHz sampling rate. The system included floating potential probes, double probes for T_e measurement, and Mach probes for velocity measurements. Radial and poloidal electric fields were derived from potential differences, enabling calculation of fluctuation-induced particle flux $\Gamma_{r,fluc}$.

3. INWARD PARTICLE FLUX OBSERVATIONS

Figure 2 shows the evolution of key plasma parameters. A remarkable transport reversal occurs after 1.3 s, with $\Gamma_{r,fluc}$ transitioning from outward to inward direction. Three distinct phases are identified: Outward flux phase (before ~1.15 s); Transport-suppressed phase (1.15-1.3 s); Inward flux phase (after 1.3 s, peaking at 1.35s).

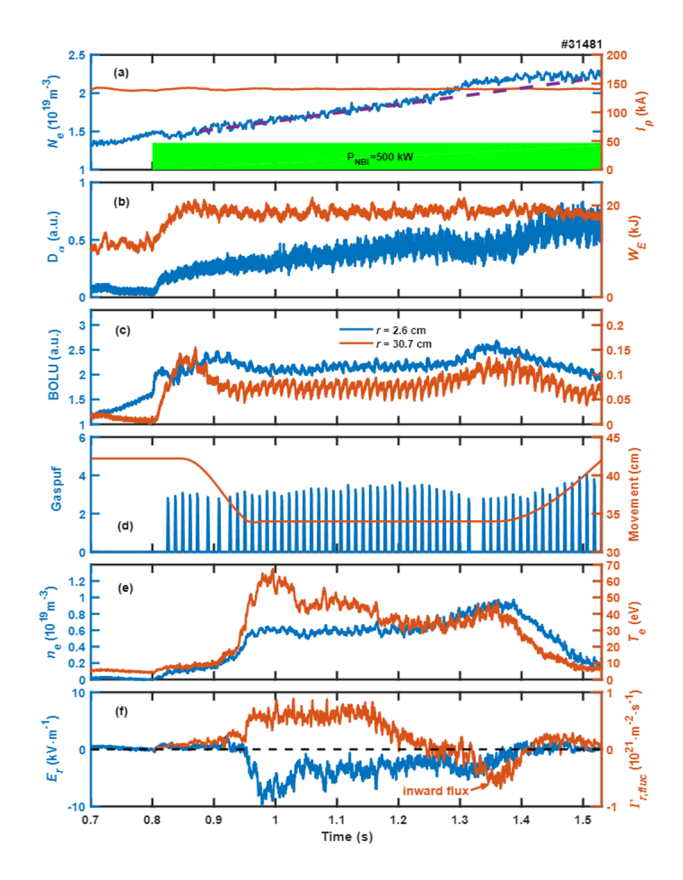


FIG. 2. Temporal evolution of (a) line-averaged density N_e , (b) D_α signal, (c) bolometer signal, (d) gas puffing and probe position, (e) edge n_e and T_e , (f) E_r and $\Gamma_{r,fluc}$.

The flux reversal coincides with accelerated density increase and reduced D_{α} signal, indicating plasma selforganization rather than external fueling. Notably, the radial electric field evolution doesn't temporally coincide with flux reversal, suggesting other factors govern transport direction.

Comparative analysis of discharges with identical parameters reveals contrasting transport behaviors (Fig. 3). The directional reversal is uniquely governed by cross-phase α_{nV} evolution, with cos α_{nV} transitioning from +1 to -1. Coherence γ_{nV} shows a 'high-low-high' pattern correlated with transport phases, while fluctuation amplitudes show negligible differences.

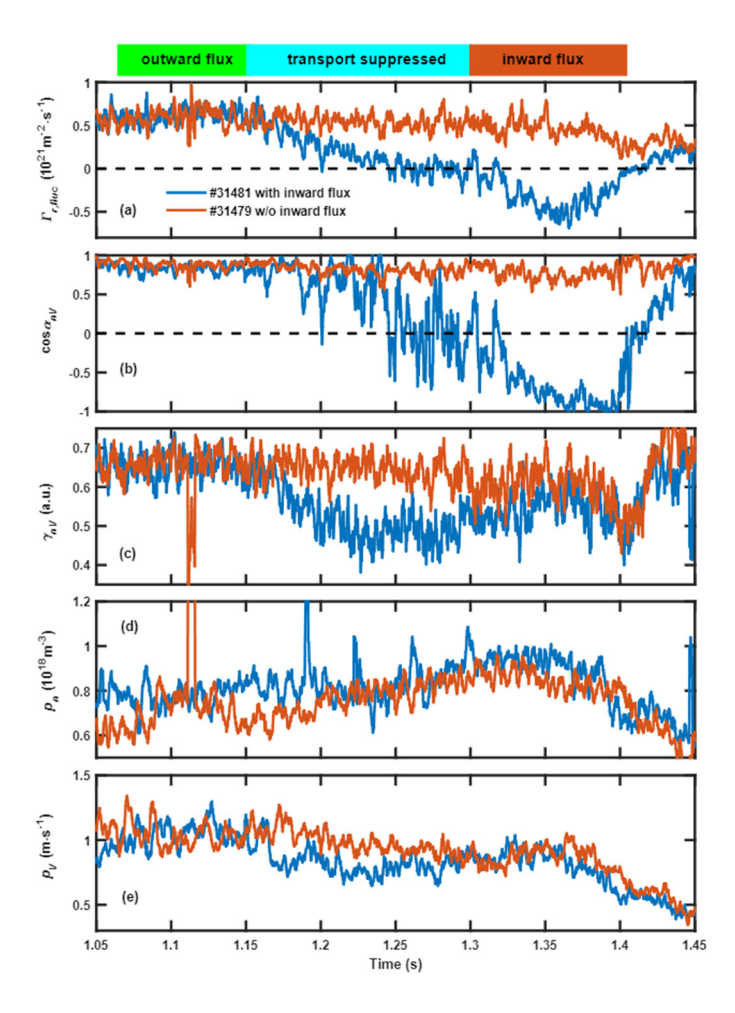


FIG. 3. Temporal evolution of (a) $\Gamma_{r,fluc}$, (b) $\cos \alpha_{nV}$, (c) γ_{nV} , (d,e) p_n and p_V for shots with/without inward flux.

Frequency-resolved analysis (Fig. 4) shows directional reversal in cos α_{nV} below 100 kHz during inward flux phase. Density fluctuations increase below 30 kHz, while velocity fluctuations show complex behavior with increase below 10 kHz but decline above 20 kHz.

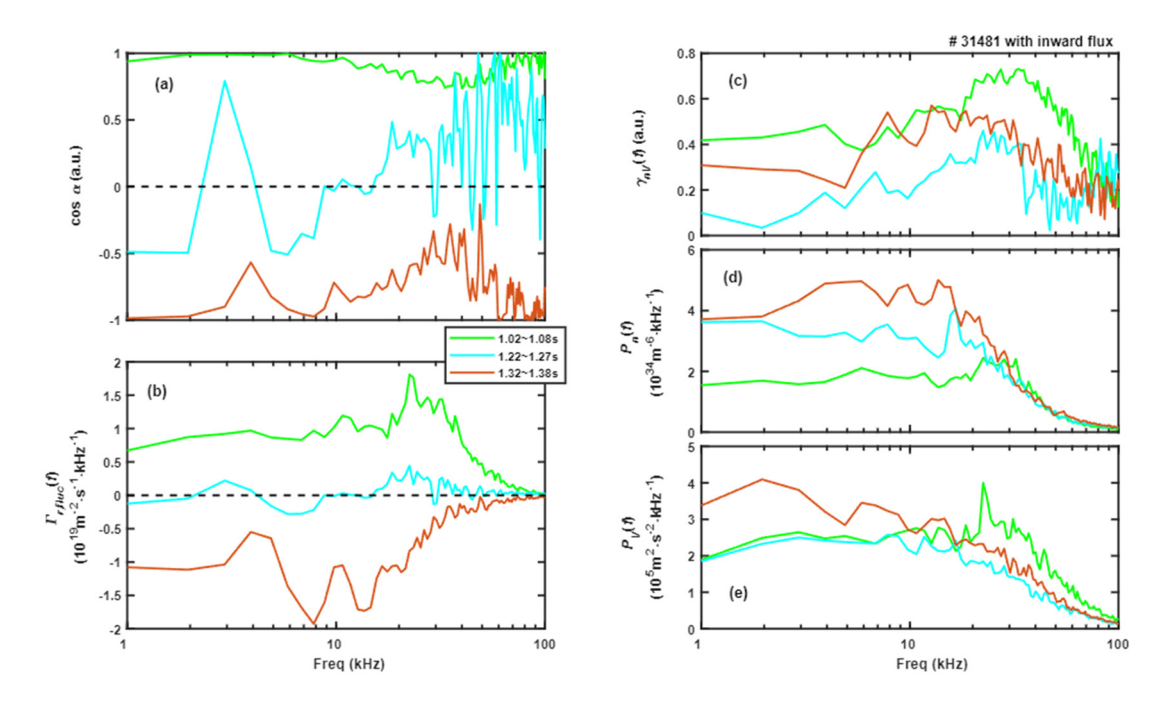


FIG. 4. Frequency-resolved (a) $\alpha_{nV}(f)$, (b) $\Gamma_{r,fluc}(f)$, (c) $\gamma_{nV}(f)$, (d) $P_n(f)$, (e) $P_V(f)$ for three transport phases.

4. TURBULENCE SPATIAL STRUCTURE

Time-frequency analysis (Fig. 5) reveals that during transport-suppressed phase, inward and outward flux coexist across different frequency bands. Strong correlations between velocity and density fluctuations occur during both outward and inward flux phases, with low correlation during suppression phase.

Wave number analysis shows significant contraction of turbulent spectra during inward transport. Fluctuations below 30 kHz exhibit: (a) Shift of k_{θ} toward near-zero values, enhancing poloidal coherence; (b) Convergence of k_r toward zero, indicating radially coherent structures; (c) Extended correlation lengths in both directions.

This organized turbulence state with reduced diffusion facilitates inward particle flux by strengthening coupling between density and velocity fluctuations. The observations suggest an inverse energy cascade mechanism, where energy transfers from small-scale, high-frequency fluctuations to larger scales and lower frequencies.

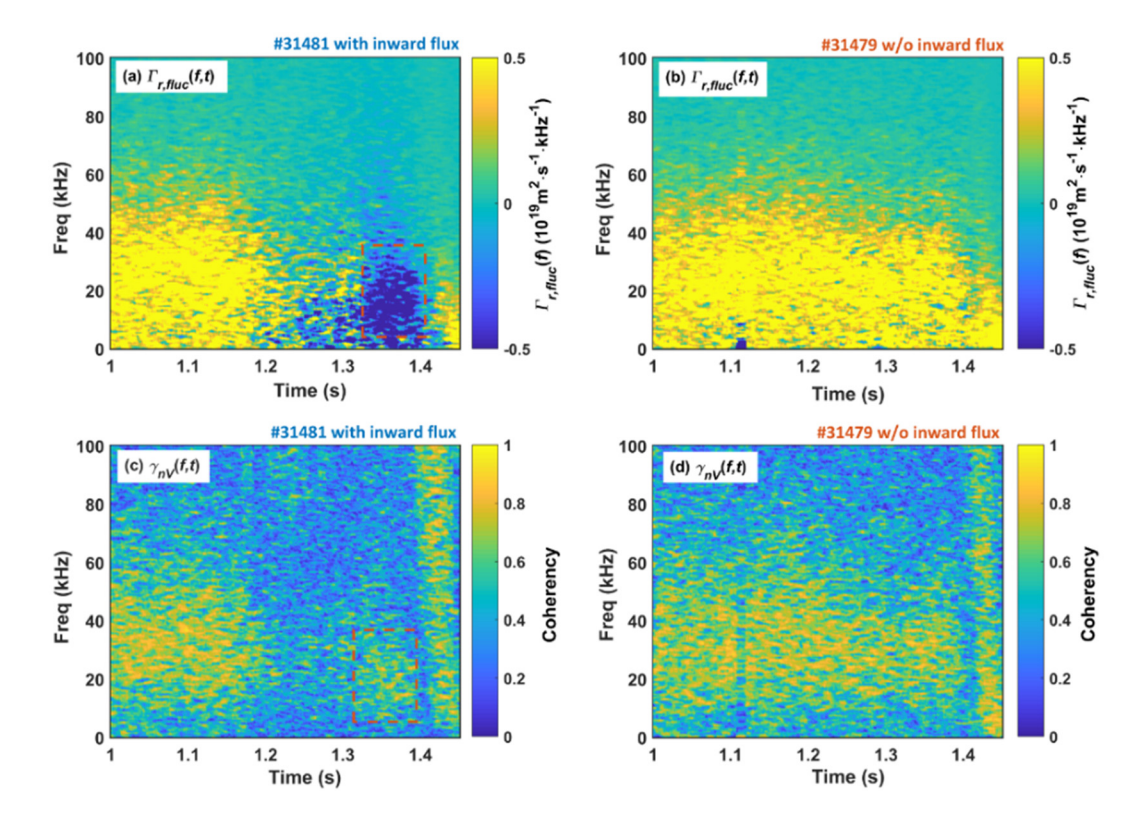


FIG. 5. Time-frequency spectra of $\Gamma_{r,fluc}$ and γ_{nV} for discharges (a,c) with and (b,d) without inward flux.

5. DRIVING MECHANISM FOR INWARD FLUX

Reynolds stress ($RS = \langle \tilde{V_r} \tilde{V_\theta} \rangle$) plays a fundamental role in turbulence dynamics. In magnetized plasmas:

$$RS \approx -\frac{1}{B_{\phi}^2} \langle \tilde{E}_{\theta} \tilde{E}_r \rangle = -\frac{1}{B_{\phi}^2} \langle k_{\theta} k_r \rangle \, |\, \tilde{\phi} \,|^2 \propto \langle k_{\theta} k_r \rangle.$$

Figure 6 shows significant divergence in Reynolds stress and radial velocity gradient evolution between discharges with and without inward transport. Key observations: (a) Reynolds stress increases before peak inward flux in inward-transport discharges; (b) Radial velocity gradient dV_r/dr increases significantly after 1.15 s; (c) Clear threshold at $dV_r/dr = 0.4 \times 10^{-6}$ s⁻¹ for flux reversal; (d) Nearly linear relationship between dV_r/dr and $\Gamma_{r,fluc}$.

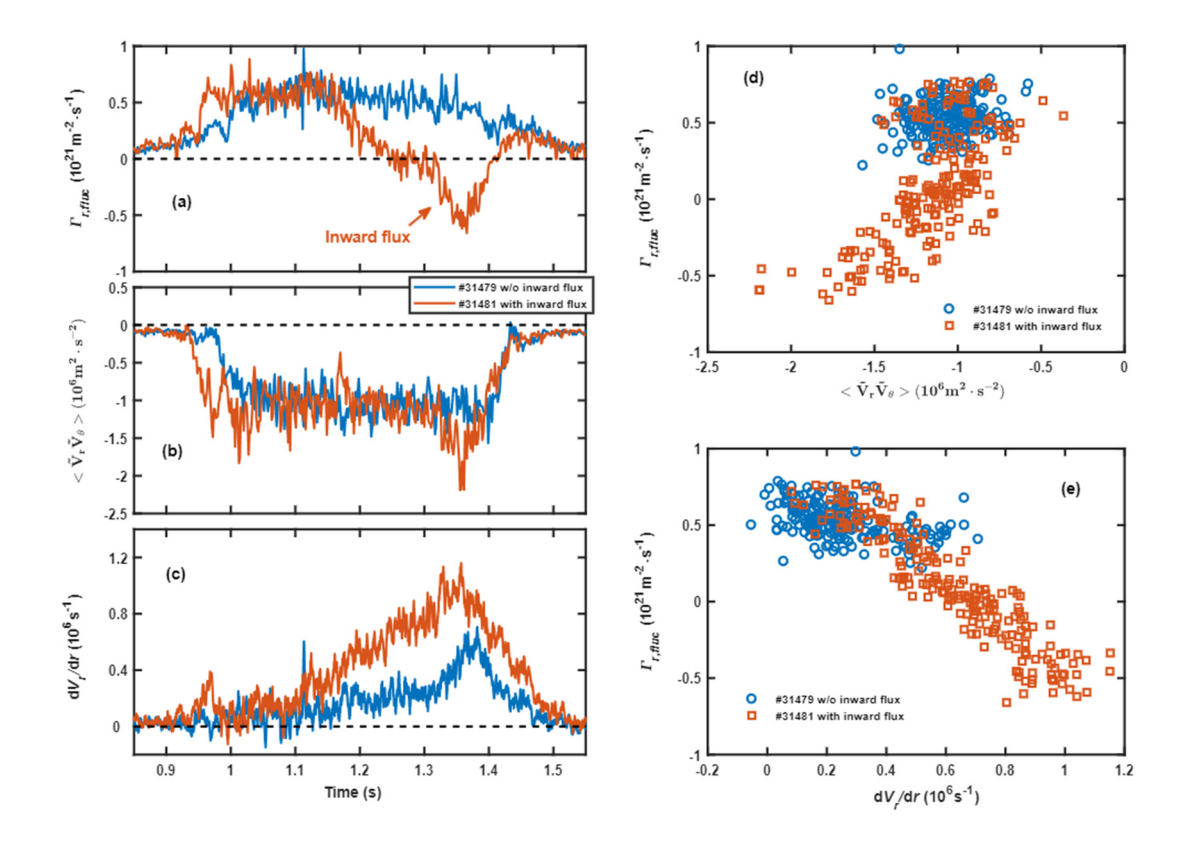


FIG. 6. Temporal evolution of (a) $\Gamma_{r,fluc}$, (b) Reynolds stress, (c) dV_r/dr , and their correlations (d,e).

Frequency decomposition reveals Reynolds stress enhancement below 40 kHz during inward flux phase (Fig. 7). The coherency $\gamma_{VrV\theta}$ increases significantly in low-frequency domain, indicating enhanced cross-dimensional correlation between radial and poloidal velocity fluctuations.

The genesis of inward flux requires not just long-range correlation in individual directions, but robust interplay between radial and poloidal components. This organized turbulence structure facilitates inverse energy transfer, sustaining inward transport against natural pressure gradients.

6. SUMMARY AND DISCUSSION

6.1. Summary

Our study demonstrates broadband fluctuation-induced inward particle transport at HL-2A plasma edge, characterized by: (a) Gradual transition from broad-spectrum outward flux to narrow-spectrum inward flux; (b) Significant density fluctuation variations with stable radial velocity fluctuations; (c) Distinct coherence evolution: high-low-high pattern correlated with transport phases; (d) Enhanced turbulence spatial coherence with extended correlation lengths; (e) Crucial roles of Reynolds stress and radial velocity gradient in driving inward transport; (f) Increased Reynolds stress coherency in low-frequency domain, indicating cross-dimensional turbulence organization.

6.2. Discussion

Cross-correlation analysis reveals that phase shifts in radial velocity fluctuations primarily drive transport direction changes, while density fluctuation amplitudes modulate flux magnitude. This separation of roles highlights the multifaceted nature of plasma transport dynamics. The enhanced coherence observed during inward flux phase resembles organized systems in nature, such as hurricane dynamics where radial-poloidal coupling maintains energy and momentum. Similarly, in tokamak plasmas, cross-dimensional turbulence coherence appears essential for driving inward particle flux against expected gradients. These findings suggest that modulating turbulence spectral content and enhancing cross-dimensional coherence could provide strategies for controlling transport direction and optimizing plasma confinement in fusion devices.

ACKNOWLEDGEMENTS

This work is supported by the National Magnetic Confinement Fusion Science Program of China (2024YFE03130003, 2022YFE03100004, 2022YFE03060003), NSFC (12405268, 12175227, 11875255, 12375226, 11975231), China Postdoctoral Science Foundation (2022M723066), Fundamental Research Funds for Central Universities (WK2140000016), and Collaborative Innovation Program of Hefei Science Center, CAS (2022HSC-CIP022).

REFERENCES

- [1] Carreras B A 1997 IEEE Trans. Plasma Sci. 25 1281
- [2] Boedo J et al. 2000 Nucl. Fusion 40 1397
- [3] Terry P W et al. 2003 Phys. Plasmas 10 1066
- [4] Shats M G et al. 1997 Phys. Rev. Lett. 79 2690
- [5] Xu Y et al. 2006 Phys. Rev. Lett. 97 165003
- [6] Kong D F et al. 2017 Nucl. Fusion 57 014005
- [7] Wu J et al. 2020 Phys. Plasmas 27 012304
- [8] Wu J et al. 2021 Nucl. Fusion 61 066003
- [9] Wu J et al. 2024 Nucl. Fusion 64 096031
- [10] Wu J et al. 2025 JUSTC 55 0403
- [11] Diamond P H et al. 2005 Plasma Phys. Control. Fusion 47 R35
- [12] Xu M et al. 2019 Nucl. Fusion 59 112017